Antiarrhythmic Engineering of Skeletal Myoblasts for Cardiac Transplantation

M. Roselle Abraham,* Charles A. Henrikson,* Leslie Tung, Marvin G. Chang, Miguel Aon, Tian Xue, Ronald A. Li, Brian O' Rourke, Eduardo Marbán

Abstract—Skeletal myoblasts are an attractive cell type for transplantation because they are autologous and resistant to ischemia. However, clinical trials of myoblast transplantation in heart failure have been plagued by ventricular tachyarrhythmias and sudden cardiac death. The pathogenesis of these arrhythmias is poorly understood, but may be related to the fact that skeletal muscle cells, unlike heart cells, are electrically isolated by the absence of gap junctions. Using a novel in vitro model of myoblast transplantation in cardiomyocyte monolayers, we investigated the mechanisms of transplant-associated arrhythmias. Cocultures of human skeletal myoblasts and rat cardiomyocytes resulted in reentrant arrhythmias (spiral waves) that reproduce the features of ventricular tachycardia seen in patients receiving myoblast transplants. These arrhythmias could be terminated by nitrendipine, an L-type calcium channel blocker, but not by the Na channel blocker lidocaine. Genetic modification of myoblasts to express the gap junction protein connexin43 decreased arrhythmogenicity in cocultures, suggesting a specific means for increasing the safety (and perhaps the efficacy) of myoblast transplantation in patients. **(*Circ Res*. 2005;97:159-167.)**

Key Words: arrhythmia ■ electrophysiology ■ gene therapy ■ optical mapping

Congestive heart failure is a major public health problem in the United States and, indeed, worldwide.[1] Cellular myoplasty represents a novel therapy for congestive heart failure but is fraught with potential pitfalls. Skeletal myoblasts (SkMs) are attractive donor cells for myoplasty: they have a contractile phenotype, can be harvested for autologous transplantation, and are resistant to ischemia.[2] In ongoing phase 2 clinical trials, SkMs are harvested from individual patients via muscle biopsy, grown in culture for 2 to 4 weeks, and then transplanted by injection into the heart.[3,4] Despite reports of improved contractile indices after myoblast transplantation,[3–5] enthusiasm has been tempered by their proarrhythmic effects.[3,4] In the literature, 10 of the first 22 patients to undergo autologous SkM cardiomyoplasty experienced subsequent ventricular tachycardia or sudden cardiac death, both early and late after SkM transplantation.[3,4] Currently, most myoblast transplantation protocols require administration of the potentially toxic antiarrhythmic drug amiodarone, or placement of an implantable cardioverter defibrillator before SkM transplantation.[6]

The mechanisms of ventricular arrhythmias associated with SkM cardiomyoplasty remain unknown. Reproducible arrhythmias were not reported in early animal studies (rat[7–9] and rabbit[5]), and there have been no reports of in vitro models of SkM arrhythmogenesis. Recently, Soliman et al reported more frequent and polymorphic premature ventricular contractions, couplets, triplets, longer pauses after premature atrial contractions, and bradycardic death (but not sustained ventricular tachycardia or ventricular fibrillation) after injection of myoblasts in the infarct border zone compared with central scar injection in a rabbit model.[10] Another study of myoblast injection after infarct did not yield a statistically-significant difference in the incidence of ventricular tachycardia or death between dogs receiving myoblast injections versus saline injections, possibly because of a high frequency of arrhythmias in both groups.[11] Hence, to pinpoint the role of SkM transplantation in arrhythmogenesis, we designed an in vitro model of myoblast transplantation.

Myoblasts differentiate into myotubes on injection into the heart.[7–9,12] Myotubes have a very brief action potential duration (APD),[7] lack gap junctions, and are therefore not coupled to surrounding ventricular myocytes or to each other.[7–9] In contrast, cardiomyocytes normally express high levels of the gap junction protein connexin43 (Cx43), resulting in very efficient electrical coupling of the cardiac syncytium. Hence, we hypothesized that a mixture of myoblasts and myocytes would result in slowing of conduction velocity and greatly increase tissue heterogeneities. Such inhomogeneities predispose to wave breaks and reentry, key elements of ventricular arrhythmias. Reentry occurs when an impulse

Original received December 29, 2004; revision received June 10, 2005; accepted June 13, 2005.

From the Institute of Molecular Cardiobiology (M.R.A., C.A.H., M.A., T.X., R.A.L., B.O'R., E.M.), and the Department of Biomedical Engineering (L.T., M.G.C.), Johns Hopkins University, Baltimore, Md.

Correspondence to Eduardo Marbán, Division of Cardiology, Johns Hopkins University, Carnegie 568, 600 N Wolfe St, Baltimore, MD 21205. E-mail marban@jhmi.edu

This manuscript was sent to Harry Fozzard, Consulting Editor, for review by expert referees, editorial decision, and final disposition.

*Both authors contributed equally to this work.

Circulation Research **is available at http://circres.ahajournals.org** **DOI: 10.1161/01.RES.0000174794.22491.a0**

fails to die out after normal activation and persists to reexcite the heart.[13] During reentry, the excitation wave may acquire the shape of an Archimedean spiral and is called a spiral wave. Most life-threatening ventricular arrhythmias result from reentrant activity.[14] Here we report sustained reentry, the in vitro equivalent of ventricular tachycardia, in monolayer cocultures of SkM and neonatal rat ventricular myocytes (NRVMs). We also find delayed repolarization of NRVMs in coculture, indicating a second, unanticipated, possibly proarrhythmic mechanism of SkM transplantation.

Materials and Methods

Lentivirus

The lenti-vectors pLV-CAG-GFP and pLV-CAG-Cx43-IRES-GFP were generated from second-generation lentiviral vector, pLV-CAG SIN-18 (Trono laboratory) under the control of the promoter CAG. Recombinant lentiviruses were generated by cotransfecting HEK293T cells with the plasmids pLV-CAG-GFP or pLV-CAG-Cx43-IRES-GFP (rat Cx43, kind gift from Mario Delmar, Syracuse, NY), pMD.G, and pCMVΔR8.91 using Lipofectamine 2000 (Invitrogen). Lentiviral particles were harvested at 24 and 48 hours after transfection and titered by FACS analysis. For transduction, lentiviruses were added to the myoblasts (MOI=10), with 8 μg/mL polybrene to facilitate transduction. Lentiviral transduction was confirmed by examining GFP expression under fluorescence microscopy (Nikon) and by immunostaining and Western blot for Cx43.

Immunostaining

Cells were fixed with 4% paraformaldehyde for 5 minutes at room temperature and then permeabilized with 0.075% saponin. Cx43 was detected using a monoclonal mouse anti-Cx43 antibody (Chemicon) and an Alexa Fluor-conjugated secondary antibody. Images were recorded using a 2-photon laser scanning microscope (Bio-Rad MRC-1024MP) with excitation at 740 nm (Tsunami Ti:Sa laser, Spectra Physics). The red emission was collected at 605±25 nm and the green emission at 525±25 nm. Images were analyzed offline using ImageJ software (Wayne Rasband, National Institutes of Health) with customized plug-ins.

Western Blot

Cells were lysed for 30 minutes on ice in lysis buffer (6 mol/L Urea, 1% SDS, 20 mmol/L Tris, 1:1000 protease inhibitor [Sigma], 0.1 mmol/L PMSF) and then centrifuged for 10 minutes at 4000 rpm. Equivalent samples (5 μg of protein, confirmed by coprobing for calsequestrin) were loaded for gel electrophoresis on 10% PAGE. After transfer to nitrocellulose, membranes were blocked and probed overnight at 4°C with primary antibodies for Cx43 (Chemicon Intl, 1:500 dilution). Membranes were incubated with horseradish peroxidase–conjugated secondary antibodies (Amersham Biosciences; 1:1000 dilution) for 1 hour at room temperature. Protein levels were detected by chemiluminescence and auto-radiography.

Calcium Transient Imaging

NRVMs and SkM were cultured on 35-mm glass-bottom microwell dishes (MatTEK Corp) for 7 days. Cultures with spontaneous beating were used for calcium transient imaging. Cells were incubated with 3 μmol/L Rhod-2 AM (Molecular Probes) for 30 minutes at 37°C. The cells were then washed 3 times and the medium was replaced, after which they were incubated for an additional 60 minutes at 37°C to allow deesterification of the Rhod-2. Isoproterenol 10 nM was added before imaging. Fluorescence imaging was performed at 37°C using an inverted fluorescence microscope (TE-2000, Nikon) with a cooled CCD camera attachment (Micro Max, Roper Scientific) using WinView32 acquisition software (Roper Scientific). GFP was imaged with 465 to 495 nm fluorescence excitation and 515 to 555 nm emission. Rhod-2 was imaged with 528 to 553 nm excitation and 578 to 633 nm emission. Ionomycin, 5 μmol/L (Calbiochem) was added at the end of the experiment to confirm uniform loading of Rhod-2.

Dye Transfer

Coupling via gap junctions was assessed by dye transfer[15] of Calcein between Cx43-transduced human skeletal myoblasts and NRVMs. The principle of the assay is as follows: Nonfluorescent Calcein-AM readily diffuses into cells across the cell membrane. Once in the cytoplasm, it is cleaved by endogeneous esterases to produce fluorescent Calcein that cannot diffuse across the cell membrane, but can be transferred between cells via Cx43 gap junctions. Briefly, myoblasts transduced with a lentivirus expressing GFP and Cx43 were grown in tissue-culture flasks, differentiated into myotubes by growing in 2% serum to confluence, and then labeled with 5 μmol/L calcein AM (Molecular Probes) for 15 to 30 minutes in a 5% CO_2 incubator at 37°C, washed with phosphate buffered saline, and then returned to the incubator for 2 hours to allow deesterification of the dye. Myoblasts were then trypsinized, centrifuged, and the pellet was suspended in culture medium and added to a monolayer of NRVMs and returned to the incubator for 3 hours by which time 30% of the cells attached. Transmitted light and fluorescence imaging were performed using an inverted fluorescence microscope (TE-2000, Nikon) with a cooled CCD camera attachment (Micro Max, Roper Scientific) using WinView32 acquisition software (Roper Scientific). Calcein was imaged with 465 to 495 nm fluorescence excitation and 515 to 555 nm emission.

Cell Culture

Human skeletal myoblasts were obtained from Cambrex (Walkersville, Md) and grown in myoblast basal growth medium (SkBM, Clonetics) containing 10% fetal bovine serum, recombinant human epidermal factor (10 ng/mL), dexamethasone (3 μg/mL), L-glutamine, gentamicin, and amphotericin–B, at 37°C and 5% CO_2 (Vials obtained from Cambrex contained 70% to 80% myoblasts, and the remainder were fibroblasts). The cells were seeded at 3500 cells/cm^2 and maintained at cell densities of 60% to 70% to prevent myotube formation during the culture process. Cells were transduced with lentivirus on their second passage and frozen at −80°C or amplified up to 10 population doublings. For cocultures, myoblasts were dissociated using trypsin, counted and then used.

Cardiac Myocytes

NRVMs were dissociated from ventricles of 2-day-old neonatal Sprague-Dawley rats (Harlan, Indianapolis, Ind) with the use of trypsin (US Biochemicals) and collagenase (Worthington) as previously described.[16] The investigation conforms to the protocols in the National Institutes of Health, *Guide for the Care and Use of Animals* (NIH publication No. 85-23, Revised 1996). Cells were resuspended in M199 culture medium (Life Technologies), supplemented with 10% heat-inactivated fetal bovine serum (Life Technologies), differentially preplated in two 45-minute steps, and then counted using a hemocytometer. For control experiments, 10^6 cells were plated (as isotropic monolayers) on 21-mm plastic coverslips coated with fibronectin (25 μg/mL); on day 2 after cell plating, serum was reduced to 2%. From our experience, reentrant arrhythmias cannot be induced in isotropic, confluent, NRVM cell cultures by rapid pacing. However, nonsustained reentries can be induced using S1-S2 protocols[16] or by using anisotropic cultures plated on patterned coverslips.[17]

Cocultures

Myoblasts and NRVMs were cocultured (as isotropic monolayers) on 21-mm plastic cover slips (coated with human fibronectin, 25 μg/mL (BD Biosciences) for 9 to 11 days and then used for optical mapping. (Neonatal rat ventricular myocytes mature to form rod-shaped, striated cells after 7 days in culture.) In an initial set of experiments, 0.5×10^6 NRVMs were plated over half of the cover slip, with the other half covered by a PDMS (polydimethylsiloxane) stamp coated with fibronectin (50 μg/mL). The PDMS stamp was removed 24 hours later and 0.5×10^6 myoblasts transduced with

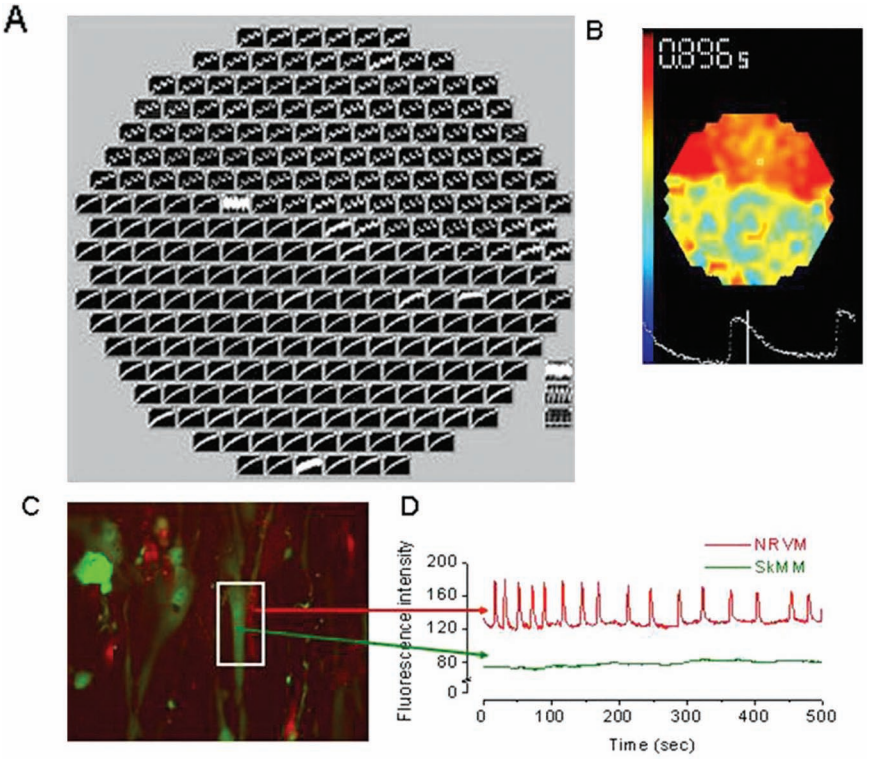

Figure 1. Myoblast:myocyte signal propagation. Optical action potentials (A) and voltage maps (B) during 2 Hz pacing of myoblast:myocyte cocultures plated with myocytes on the top half and myoblasts on the bottom half show conduction block at the SkM:NRVM interface. Color bar shows pseudocoloring of optical traces normalized from resting level (blue) to action potential peak (red). Islands of apparent activation in myoblast half of cover slip are artifacts attributable to the normalization procedure. Action potential trace at bottom was recorded at site in the map marked by a small white square. Fluorescent microscopy images (GFP positive myoblasts in green and myocytes in red; C) and calcium transient recordings of myoblast-:myocyte cocultures (D) show lack of propagation of calcium transients from myocytes to neighboring myotubes.

Lv-GFP were then plated. This experiment was performed to ascertain whether or not there is electrical propagation between NRVMs and myotubes at a syncytial level. In a second set of experiments, the myoblasts (transduced with LvGFP) and NRVMs were plated at the same time in varying ratios: 1:1, 1:4, and 1:9 to study the electrophysiologic consequences of mixing the 2 cell types.

On day 2 after cell plating, serum was reduced to 2%. An additional set of experiments (n=3) was performed in 1:4 (non GFP-transduced) myoblast:myocyte cocultures. Finally, myoblasts transduced with Lv-Cx43 were cocultured with NRVMs in ratios of 1:1 and 1:4.

HeLa cells, a human cervical carcinoma cell line that lacks Cx43,[18] were obtained from ATCC and cultured in Dulbecco's Modified Eagle Medium (Invitrogen) supplemented with 10% heat-inactivated fetal bovine serum (Hyclone) and 2 mmol/L glutamine. Cells were expanded, trypsinized, and then cocultured with NRVMs in ratios of 1:4, 1:9, and 1:99. Optical mapping was performed after only 5 days in culture because of the high proliferative rates of HeLa cells. Given the high proliferative rate of HeLa cells, cocultures containing 10% and 20% HeLa cells at plating were inexcitable by day 5 because of small numbers of NRVMs. Cocultures containing 1% HeLa cells at initial plating contained 30% to 40% HeLa cells by day 5 of coculture and could be electrically stimulated.

Optical Mapping

Coverslips were visually inspected under a microscope. Monolayers with obvious gaps in confluence and nonbeating cultures were rejected. The coverslips were placed in a custom-designed chamber, stained with 5 μmol/L di-4-ANEPPS (Molecular Probes) for 5 minutes, and continuously superfused with warm (36.5°C) oxygenated Tyrode solution consisting of (in mM) 135 NaCl, 5.4 KCl, 1.8 $CaCl_2$, 1 $MgCl_2$, 0.33 NaH_2PO_4, 5 HEPES, and 5 glucose. A unipolar point or area electrode (4 parallel bipolar-line electrodes) was used to stimulate the cells in culture. Action potentials were recorded using a custom-built contact fluorescence imaging system modified to have 253 recording sites.[15] The recording chamber was placed directly above a fiber bundle with fibers arranged in a 17-mm-diameter hexagonal array. A light emitting diode (LED) light source with an interference filter (530±25 mm) delivered excitation light to the chamber. A Plexiglas cover was placed on top of the chamber to stabilize the solution surface and reduce optical artifacts. The bottom of the chamber consisted of a No. 1 circular glass coverslip spin-coated with 3 layers of red ink (Avery Dennison) to attenuate the excitation light and pass the red emission signal. Optical signals were low-pass filtered at 500 Hz and amplified with 8 custom-designed 32-channel printed circuit boards. Signals were sampled at 1 kHz and digitized with 4, 64 channel 16 bit analog-to-digital

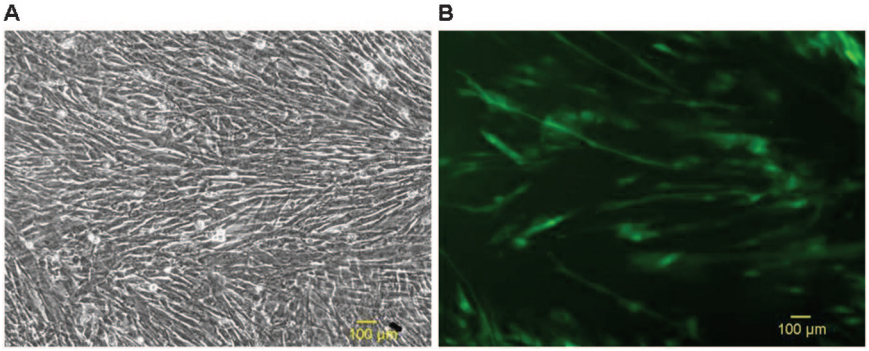

Figure 2. A and B, Imaging of SkM-NRVM cocultures. A, Transmitted light image of a 1:4 SkM-NRVM coculture shows a confluent monolayer. B, Fluorescent image of Lv-GFP transduced SkM in coculture with NRVMs in ratio of 1:4 shows a random irregular distribution of myotubes.

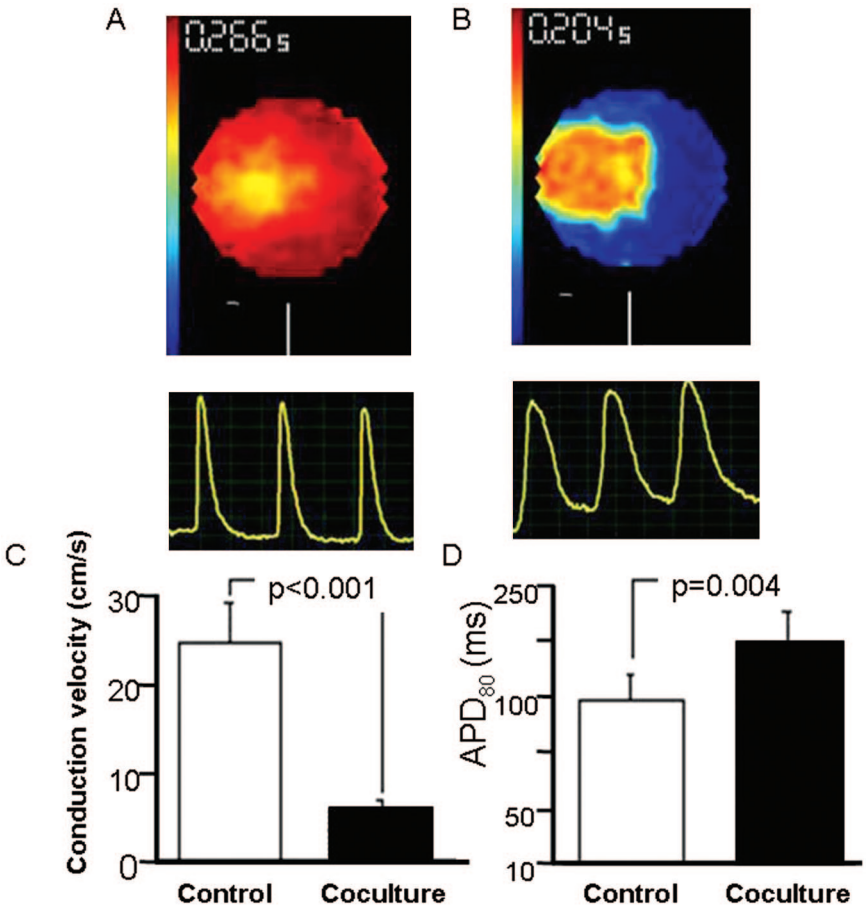

Figure 3. A and B, Impulse propagation. Voltage maps and optical action potentials during propagation of an impulse 50 ms after the stimulus in NRVM-only monolayer control (A) and a representative 1:4 Lv-GFP coculture (B). The propagation wavefront is irregular in the coculture, and propagation is very delayed compared with control. Color bar in figure corresponds to normalized voltage level, with blue being the resting state and red being peak of action potential. Traces are representative optical action potentials measured in the monolayers. Bar graphs display conduction velocity (C) and APD_{80} (APD at 80% of repolarization; D) in NRVM-only controls (n=7) and 1:4 LvGFP cocultures (n=6). Conduction velocity is significantly decreased ($P<0.001$), whereas APD_{80} is significantly increased ($P=0.004$) in cocultures containing Lv-GFP-transduced myoblasts compared with controls.

boards (Sheldon Instruments). Data were stored, displayed, and analyzed using software written in Visual C++ (Microsoft), Laboratory VIEW (Texas Instruments), and MATLAB (Math Works).

Experimental Protocol

A 1-s recording was initially made to check for spontaneous activity. Fifteen beat drive trains of 10 ms monophasic pulses (1.5X diastolic threshold) were subsequently used for stimulation throughout the experiment. Stimulation was begun at 1 Hz and increased progressively by 1 Hz until 1:1 capture was no longer observed, or reentry was initiated. Nitrendipine (5 μmol/L) or lidocaine (200 μmol/L) in warm (36.5°C) Tyrode solution was superfused into the experimental chamber and 2-sec recordings were obtained every 30 to 60 sec for 10 minutes or until termination of reentry. The drug was then washed out over 10 minutes with drug-free Tyrode solution, and another recording was obtained. If reentry was terminated, stimulation was begun at 1 Hz and increased as before. If reentry was not terminated or if reinitiated, a second drug was introduced. We found that nitrendipine (5 μmol/L) shortened APD by 50% but did not affect conduction velocity in NRVM-only cultures (see online Figure I, available at http://circres.ahajournals.org). Higher doses of nitrendipine produce Na channel blockade in addition to L-type calcium channel blockade.[19]

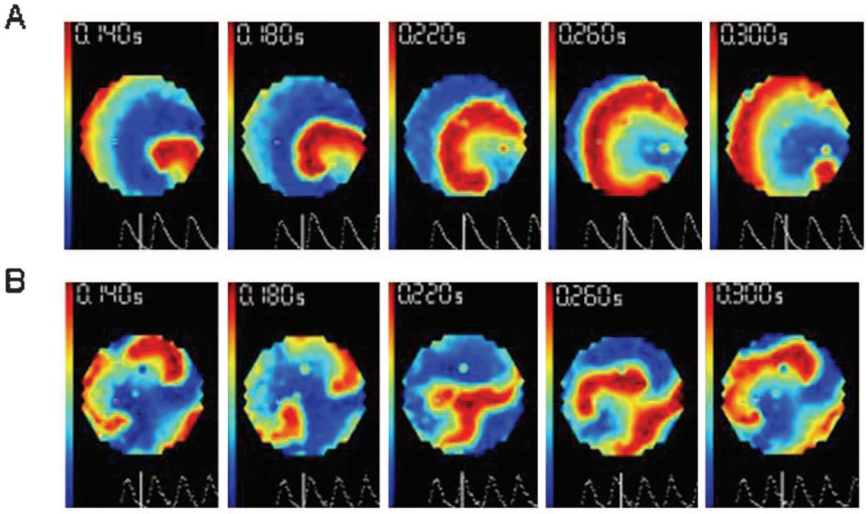

Figure 4. Patterns of reentry. Voltage maps during reentry in two 1:4 Lv-GFP:NRVM cocultures showing single spiral (a) and figure-of-8 spiral (b). (The color bar in the figure is the same as in Figure 3.)

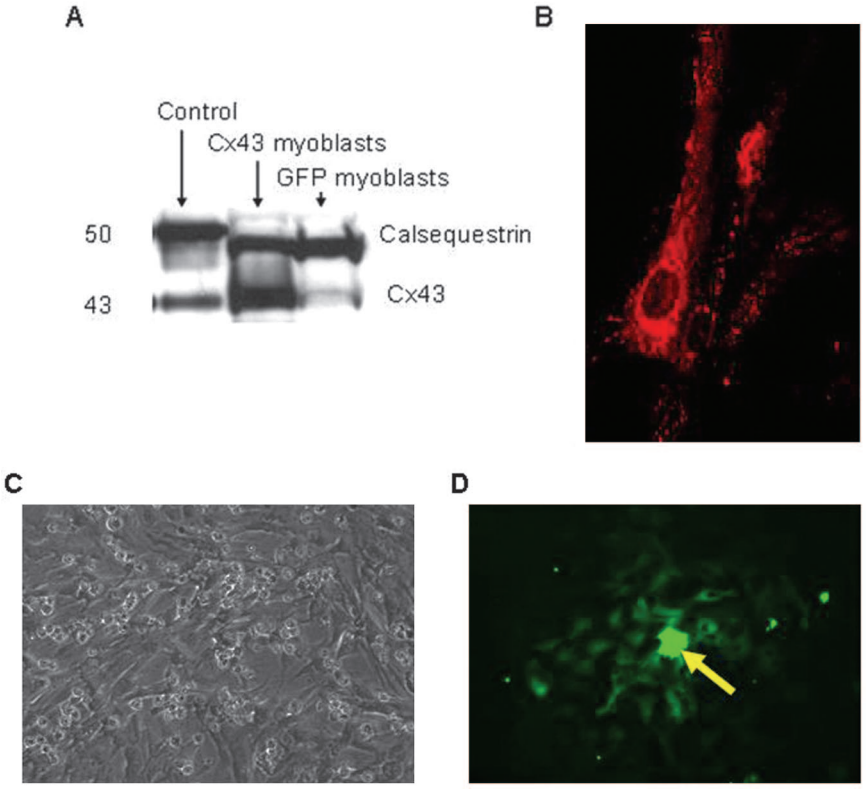

Figure 5. Overexpression of Cx43 in myoblasts. A, Western blot analysis of Cx43 and calsequestrin expression in ventricular myocytes (control), Lv-Cx43-expressing myoblasts and Lv-GFP-expressing myoblasts. B, Fluorescent images of Cx43 expression in Cx43-transduced myoblasts. C and D, Dye transfer of Calcein between Cx43-transduced SkM and neonatal rat ventricular myocytes. C, transmitted light image and (D) fluorescent microscopy image of dye transfer from a Cx43-transduced myotube to neighboring NRVMs and between adjacent NRVMs. Arrow indicates Cx43-transduced SkM loaded with Calcein.

Data Analysis

Baseline drift was reduced by subtraction of a fitted polynomial curve from the optical signal. Animations of electrical propagation were generated from signals that were band-pass filtered between 0 and 100 Hz. The activation time was defined as the instant of maximum positive slope. Cocultures with a myoblast:myocyte ratio of 1:4 during the plating step were used for analysis of CV and APD. The relative activation times at each recording point of the hexagonal array were used to calculate conduction velocity. To compare velocities among different episodes in the same monolayer, conduction velocity was calculated along the same path and averaged over different stimulus responses. Paths were chosen to be sufficiently far away from the stimulus site so that latency delays associated with excitation could be neglected.

Statistics

Data are expressed as mean±SD unless stated otherwise. Differences between means were assessed using the Student *t* test or Fischer exact test.

Results

Absence of Electrical Coupling Between Myotubes and Myocytes

One likely contributor to arrhythmias after myoblast transplantation in humans is the predicted absence of electrical coupling between NRVMs and myotubes. Indeed, mathematical simulations have shown that, with decreased gap junction coupling, conduction is very slow but, paradoxically, very robust (because of an increase in the safety factor for propagation),[20] increasing the tendency for reentry.[17] We confirmed the lack of electrical coupling at a syncytial level by optical mapping of cocultures plated with SkMs on one half and NRVM on the other half of the coverslip (n=6). Stimulation on the NRVM half resulted in a propagated wave front that blocked at the NRVM/SkM interface (Figure 1A and 1B). The absence of electrical coupling was confirmed at a single-cell level by measuring lack of propagation of calcium transients between neighboring myocytes and myotubes using Rhod-2 AM (5 μmol/L) as the calcium indicator. (Figure 1C and 1D; n=20)

Optical Mapping of Cocultures

To examine the electrophysiologic consequences of mixing myoblasts and cardiomyocytes, we next proceeded to characterize mixed cocultures, a situation that mimics the engraftment of SkMs in hearts in vivo.[12,21] Light (Figure 2A) and fluorescence microscopy (Figure 2B) revealed that myotubes tend to grow in linear irregular patterns. We also found that plating of 10% or 20% SkMs resulted in 30% to 40% SkMs after 7 days in culture because myoblasts continued to divide in culture before fusing to form myotubes. The electrically-uncoupled myotubes interspersed among NRVMs would be expected to behave as localized barriers to propagation, resulting in slowing of overall conduction and a predisposition to irregularities in the wave front, source-load mismatch, wave break and reentry.[18,22,23] Indeed, optical mapping of mixed SkM/NRVM cocultures revealed greatly decreased conduction velocity, compared with control (NRVM-only) cultures. (Figure 3A, 3B, and 3C) show conduction velocity in cocultures compared with control. Additionally, APD_{80} in cocultures was prolonged (Figure 3B and 3D). The latter finding was unanticipated but, if present in vivo, could contribute to arrhythmogenesis by inhomogenous alterations of repolarization.[24]

In cocultures, but not in controls, the depolarization wavefront was irregular (Figure 3B), with wave breaks occurring

at pacing rates of 4 to 6 Hz and preceding reentry initiation. Additionally, lack of 1:1 conduction developed at a pacing rate of 4 to 6 Hz in cocultures, but only at a high pacing rate of 8 to 11 Hz in NRVM controls.

Reentrant rhythms (spiral waves) were easily inducible by rapid pacing in 100% of the mixed cocultures (n=28; SkM:NRVM ratios of 1:1 [n=7], 1:4 [n=14], and 1:9 [n=7]). In contrast, reentry could not be induced in NRVM-only controls (n=7) or in cocultures containing 1% SkMs. In one 1:4 coculture, spontaneous reentry was present before pacing. The spontaneous and induced reentrant rhythms (Figure 4A and 4B) were varied: single, multiple, or figure-eight (2 counter-rotating spirals) spirals that were stable, drifting, or transient.

Most (90%) of the induced reentrant arrhythmias were stable and sustained for >5 minutes, making them amenable to pharmacological intervention. High doses of lidocaine (200 μmol/L), a Na channel blocker and commonly used antiarrhythmic, slowed the reentry rate by 70% to 80% but did not terminate it in the majority of cocultures (n=12). In contrast, nitrendipine (5 μmol/L), an L-type calcium current (I_{CaL}) blocker, slowed the reentrant rhythms by a modest 10% to 20% before abrupt termination (n=12) in all cocultures. The observed dependence of propagation on I_{CaL} provides further support for the notion that decreased gap junction coupling underlies the decrease in conduction velocity and increase in inducibility of reentry in cocultures. In fact, mathematical modeling[20] and experimental data[18] have shown that, with decreased gap junction coupling, conduction delays between cells or groups of cells markedly exceed the rise time of the action potential upstroke, making propagation increasingly dependent on I_{CaL} rather than Na current.

Connexin43 Expression in Myotubes Is Antiarrhythmic

Pharmacotherapy with calcium channel blockers in patients with heart failure is limited by side effects such as contractile failure and hypotension.[25] As an alternative means to decrease arrhythmogenesis, we investigated genetic enhancement of cell–cell coupling by stable lentivirally-mediated transduction of SkM with Cx43. Western blot (Figure 5A) showed greatly increased Cx43 expression compared even to ventricular myocyte controls and immunostaining (Figure 5B) revealed plaques in the membrane, as well as large amounts of punctate staining in the membrane and in the cytoplasm. Gap junction function was assessed by dye transfer of calcein from Cx43-transduced myotubes into neighboring ventricular myocytes. Figure 5C and 5D shows ample transfer of calcein from engrafted Cx43-expressing SkMs to surrounding NRVMs, verifying the functional competency of expressed gap junctions

In Cx43-expressing SkM-NRVM cocultures, conduction velocity was increased by 30% and APD_{80} was decreased by 20% compared with the Lv-GFP cocultures (Figure 6 A and 6B). APD shortening is probably attributable to electrical coupling of myotubes that have brief action potentials with NRVMs. Sustained reentry was induced in 2 of 9 Cx43-transduced cocultures compared with 13 of 14 Lv-GFP-transduced cocultures (P=0.001, Fischer exact test; Figure 6C). These results show that genetic modification of SkMs to express Cx43 before transplantation suppresses arrhythmias in cocultures. Cx43 transduction of SkM, by promoting electrical coupling between myocytes and SkM, probably decreases tissue heterogeneities and hence reentry. Further in vivo studies are needed to address the role of Cx43 overex-

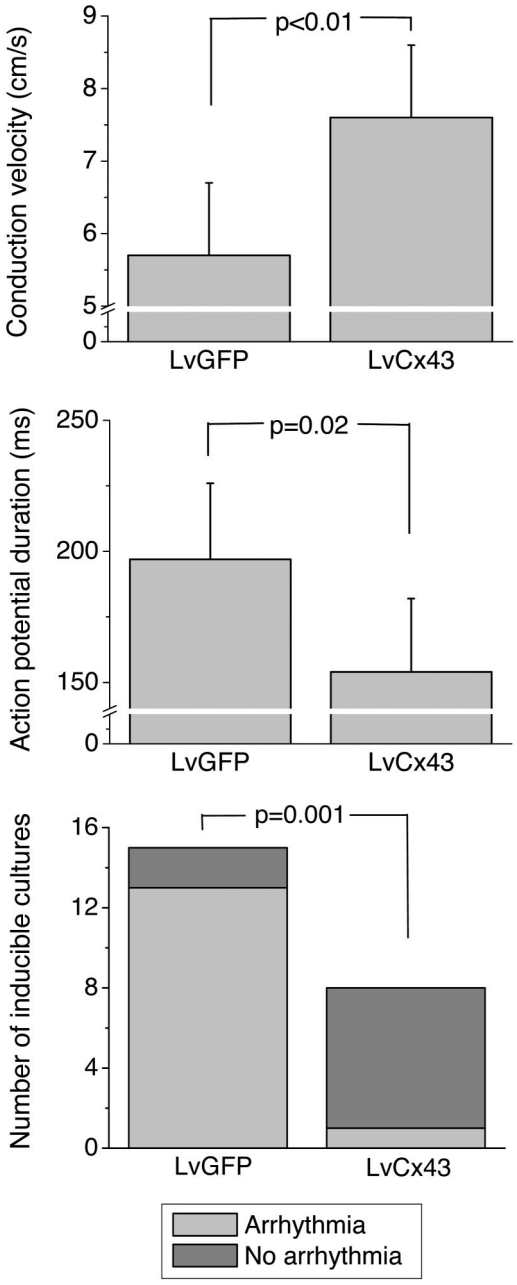

Figure 6. Changes in conduction characteristics in cocultures with Cx43 overexpression in SkMs. Bar graphs demonstrating conduction velocity (A) and APD_{80} (B) in 1:4 LvGFP (n=6) and 1:4 LvCx43 (n=6) cocultures. Conduction velocity is significantly increased (P<0.01) in Cx43 compared with GFP cocultures. Additionally, APD_{80} is significantly decreased (P=0.02) in cocultures containing Lv-Cx43-transduced myoblasts. C, Bar graphs indicate numbers of cocultures in which sustained reentry was induced. Sustained reentry was induced in 2 of 9 Cx43-transduced cocultures and 13 of 14 Lv-GFP-transduced cocultures (P=0.001, Fisher exact test).

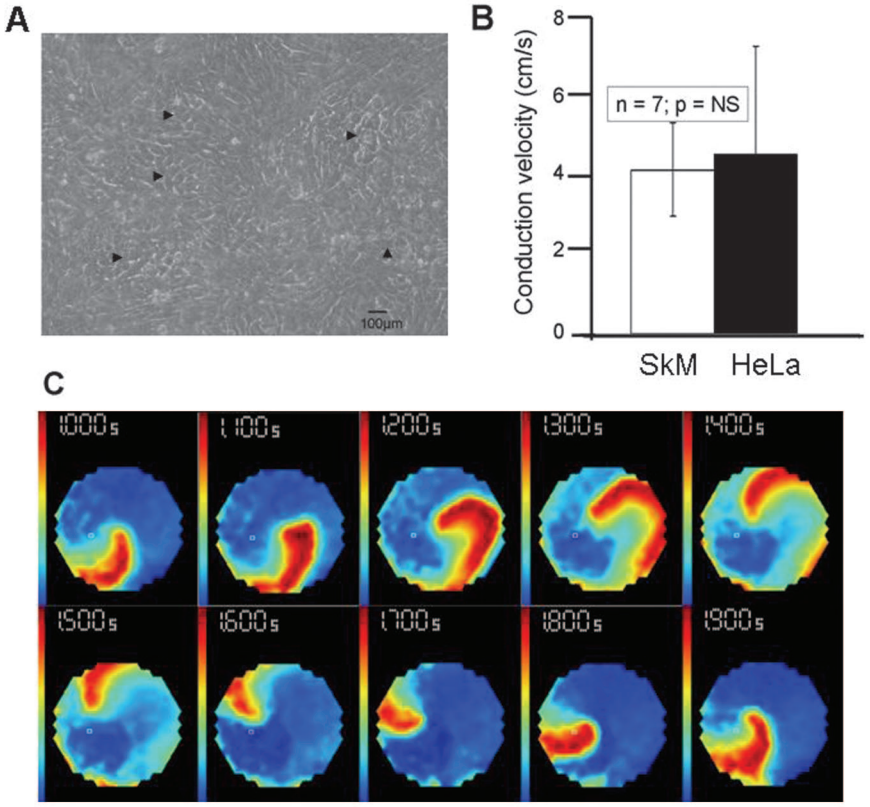

Figure 7. HeLa cocultures. A, transmitted light image of a HeLa-NRVM coculture on day 5 after plating 1% HeLa cells and 99% NRVMs; arrowheads indicate HeLa cell clusters. Bar graphs demonstrate comparison of conduction velocity between 1:4 SkM-NRVM (□) and HeLa-NRVM (■) cocultures (n=7 in each; B), voltage maps during sustained reentry in a HeLa-NRVM coculture (C).

pression in myoblast transplantation, because coupling of myocytes with myotubes that have brief action potentials may have the potential downside of increased dispersion of repolarization in the heart.

To further validate the concept that mixtures of electrically-uncoupled cells with cardiac myocytes would increase the propensity for reentrant arrhythmias, we cocultured NRVMs with HeLa cells that lack Cx43. Optical mapping of cocultures containing 30% to 40% HeLa cells (Figure 7A) showed decreased conduction velocity (Figure 7B) and irregular wavefronts, similar to those seen in Skm-NRVM cocultures. Also, reentry was inducible in 100% of cocultures that could be electrically stimulated (n=15). Surprisingly, most (14/15) of the reentries that were induced drifted to the edge of the coverslip and terminated after a few seconds, unlike the case in SkM-NRVM cocultures where reentries are typically stable and sustained for hours. (Figure 7C is an example of sustained reentry that was induced in a HeLa-NRVM coculture.) We propose that this result could be attributed to difference in tissue architecture between HeLa and SkM cocultures, highlighting the importance of tissue architecture in induction and maintenance of reentrant arrhythmias. In HeLa cocultures, the HeLa cells are polygonal and grow in clusters, producing islands (100 to 500 μmol/L in diameter) of HeLa cells (Figure 7A) surrounded by myocytes, whereas SkMs fuse to form myotubes that are long and range in length from 100 to 1500 μmol/L (Figure 2B), a feature that probably facilitates pinning of spiral waves and facilitates stable reentrant arrhythmias in 21-mm coverslips.

Discussion

Reentrant Arrhythmias

Our results provide the first in vitro demonstration of the arrhythmogenicity of myoblast transplantation and demonstrate that myoblast:myocyte interactions alone can provide the electrophysiologic milieu for reentrant arrhythmias. These findings may at least partially explain the clinical observations of high rates of ventricular tachycardia in patients who have undergone autologous SkM transplant after myocardial infarction. Injection of SkMs into the infarct border zone (characterized by fibrosis,[26] gap junction remodeling,[27] and slow conduction[28]) would be expected to further slow conduction, promote wave-breaks, and result in an increased risk of reentrant rhythms. Surprisingly, sustained ventricular arrhythmias and sudden death were not reported in early animal models of myoblast transplantation. Possible explanations for these negative results could be that the animals did not undergo detailed electrocardiographic or invasive electrophysiologic evaluation or that rodent hearts are more resistant to development of ventricular tachycardia and fibrillation because of their small heart size. An important advantage of our in vitro model is that it permits detailed electrophysiological investigation of SkM–myocyte interactions without the confounding effect of heart failure that is often present in animal models of myoblast transplantation.

Another important result is the effect of SkM number on induction of reentry. Reentry was not induced in cocultures that contained 1% to 5% myoblasts (n=7), but was consistently induced in cocultures containing greater than 20% to

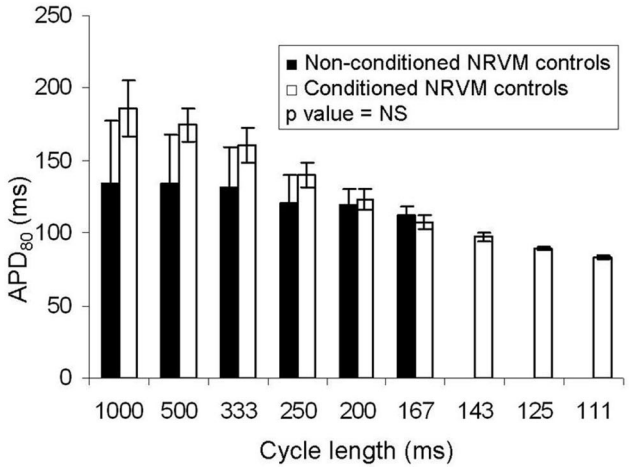

Figure 8. Effect of SkM-conditioned media on NRVM-only controls at increasing pacing frequencies (n=6 in each group). Bar graph shows increased APD_{80} in controls after treatment with conditioned media; however, results are not statistically significant.

30% myoblasts (n=28). This may explain lack of a proarrhythmic effect after transplantation of other stem cells, like bone marrow derived stem cells that are associated with low rates of engraftment. In contrast, SkM injection in animal models and humans has resulted in significant degrees of engraftment, differentiation,[21] and long-term persistence of myotubes interspersed among myocytes[12,29] which might explain the increased incidence of arrhythmias in the immediate postoperative period, as well as, in the longer term in these patients.[3,4]

Action Potential Prolongation

An unanticipated finding was the delay of cardiac repolarization that may represent a novel proarrhythmic effect[24] of SkM coculture, above and beyond the predictable slowing of conduction. APD prolongation has been associated with triggered activity in the clinical setting[30,31] and in experimental models of heart failure.[32,33] However, APD prolongation may also be antiarrhythmic by increasing wavelength and decreasing excitable gap of reentry. In our model, the antiarrhythmic effect of APD prolongation on reentry wavelength was probably offset by the proarrhythmic effect of severely depressed conduction velocity.

We hypothesize that APD prolongation may be a paracrine effect of SkMs.[34] SkMs express growth factors like insulin-like growth factor-1 (IGF-1)[35] that may promote myocyte hypertrophy and consequent APD prolongation.[36] To investigate this possibility, we cultured NRVMs in conditioned media (obtained from myoblast cultures). We found that APD was prolonged after exposure of NRVMs to conditioned media for 5 days, but the difference was not statistically significant (Figure 8).

Limitations

The main limitations of this study with respect to extrapolation of the results to humans include use of a cell culture model containing ventricular myocytes derived from neonatal rat hearts that have higher intrinsic rates, different ion channel composition, and gap junction distribution when compared with adult human myocytes. Also, the optical mapping system used in the study does not permit simultaneous recording of light microscopy and voltage signals. Hence we were unable to correlate the features of core anatomy or core location with skeletal myoblast location or density.

Conclusion

Our in vitro data demonstrate that myoblast transplantation alone may provide the substrate for reentrant ventricular arrhythmias. Because improvement in function appears to be independent of electrical integration,[21,34] based on our findings, SkM injection into scar and not the border zone could potentially prevent occurrence of reentrant arrhythmias. Cx43 transduction of myoblasts and I_{CaL} blockers could be useful adjuncts in myoblast transplantation to reduce arrhythmias.

Acknowledgments

This study was supported by the Donald W. Reynolds Foundation, the ACC Career Development Award (M.R.A.), and National Institutes of Health Grant HL66239 (L.T.). E.M. holds the Michel Mirowski, MD, Professorship of Cardiology. We thank Roland Emokpae Jr. and Pei Hong Dong for technical assistance.

References

1. Ho KK, Anderson KM, Kannel WB, Grossman W, Levy D. Survival after the onset of congestive heart failure in Framingham Heart Study subjects. *Circulation*. 1993;88:107–115.
2. Menasche P. Skeletal muscle satellite cell transplantation. *Cardiovasc Res*. 2003;58:351–357.
3. Menasche P, Hagege AA, Vilquin JT, Desnos M, Abergel E, Pouzet B, Bel A, Sarateanu S, Scorsin M, Schwartz K, Bruneval P, Benbunan M, Marolleau JP, Duboc D. Autologous skeletal myoblast transplantation for severe postinfarction left ventricular dysfunction. *J Am Coll Cardiol*. 2003;41:1078–1083.
4. Smits PC, van Geuns RJ, Poldermans D, Bountioukos M, Onderwater EE, Lee CH, Maat AP, Serruys PW. Catheter-based intramyocardial injection of autologous skeletal myoblasts as a primary treatment of ischemic heart failure: clinical experience with six-month follow-up. *J Am Coll Cardiol*. 2003;42:2063–2069.
5. Taylor DA, Atkins BZ, Hungspreugs P, Jones TR, Reedy MC, Hutcheson KA, Glower DD, Kraus WE. Regenerating functional myocardium: improved performance after skeletal myoblast transplantation. *Nat Med*. 1998;4:929–933.
6. Minami E, Reinecke H, Murry CE. Skeletal muscle meets cardiac muscle. Friends or foes? *J Am Coll Cardiol*. 2003;41:1084–1086.
7. Leobon B, Garcin I, Menasche P, Vilquin JT, Audinat E, Charpak S. Myoblasts transplanted into rat infarcted myocardium are functionally isolated from their host. *Proc Natl Acad Sci U S A*. 2003;100:7808–7811.
8. Al Attar N, Carrion C, Ghostine S, Garcin I, Vilquin JT, Hagege AA, Menasche P. Long-term (1 year) functional and histological results of autologous skeletal muscle cells transplantation in rat. *Cardiovasc Res*. 2003;58:142–148.
9. Murry CE, Wiseman RW, Schwartz SM, Hauschka SD. Skeletal myoblast transplantation for repair of myocardial necrosis. *J Clin Invest*. 1996;98:2512–2523.
10. Soliman A, Krucoff M, Crater S, Morimoto Y, Taylor D. Cell location may be a primary determinant of safety after myoblast transplantation into the infarcted heart. *J Am Coll Cardiol*. 2004:43:15A. (Abstract).
11. Sherman W, He K-L, Yi G-H, Zhou H, Gu A, Becker EM, Zhang G-P, Harvey J, Kao R, Lee M, Wang J, Haimes H, Burkhoff D. Ventricular arrhythmias following autologous skeletal myoblast implantation. *J Am Coll Cardiol*. 2003:41:176A. (Abstract).
12. Hagege AA, Carrion C, Menasche P, Vilquin JT, Duboc D, Marolleau JP, Desnos M, Bruneval P. Viability and differentiation of autologous skeletal myoblast grafts in ischaemic cardiomyopathy. *Lancet*. 2003;361:491–492.
13. Antzelevitch C. Basic mechanisms of reentrant arrhythmias. *Curr Opin Cardiol*. 2001;16:1–7.

14. Zipes DP. Mechanisms of clinical arrhythmias. *J Cardiovasc Electrophysiol*. 2003;14:902–912.
15. Zhang ZQ, Hu Y, Wang BJ, Lin ZX, Naus CC, Nicholson BJ. Effective asymmetry in gap junctional intercellular communication between populations of human normal lung fibroblasts and lung carcinoma cells. *Carcinogenesis*. 2004;25:473–482.
16. Iravanian S, Nabutovsky Y, Kong CR, Saha S, Bursac N, Tung L. Functional reentry in cultured monolayers of neonatal rat cardiac cells. *Am J Physiol Heart Circ Physiol*. 2003;285:H449–H456.
17. Bursac N, Parker KK, Iravanian S, Tung L. Cardiomyocyte cultures with controlled macroscopic anisotropy: a model for functional electrophysiological studies of cardiac muscle. *Circ Res*. 2002;91:e45–e54.
18. Rohr S, Kucera JP, Kleber AG. Slow conduction in cardiac tissue, I: effects of a reduction of excitability versus a reduction of electrical coupling on microconduction. *Circ Res*. 1998;83:781–794.
19. Yatani A, Brown AM. The calcium channel blocker nitrendipine blocks sodium channels in neonatal rat cardiac myocytes. *Circ Res*. 1985;56:868–875.
20. Shaw RM, Rudy Y. Ionic mechanisms of propagation in cardiac tissue. Roles of the sodium and L-type calcium currents during reduced excitability and decreased gap junction coupling. *Circ Res*. 1997;81:727–741.
21. Reinecke H, Murry CE. Transmural replacement of myocardium after skeletal myoblast grafting into the heart. Too much of a good thing? *Cardiovasc Pathol*. 2000;9:337–344.
22. Kucera JP, Kleber AG, Rohr S. Slow conduction in cardiac tissue, II: effects of branching tissue geometry. *Circ Res*. 1998;83:795–805.
23. Kleber AG, Rudy Y. Basic mechanisms of cardiac impulse propagation and associated arrhythmias. *Physiol Rev*. 2004;84:431–488.
24. Tomaselli GF, Beuckelmann DJ, Calkins HG, Berger RD, Kessler PD, Lawrence JH, Kass D, Feldman AM, Marbán E. Sudden cardiac death in heart failure. The role of abnormal repolarization. *Circulation*. 1994;90:2534–2539.
25. de Vries RJ, van Veldhuisen DJ, Dunselman PH. Efficacy and safety of calcium channel blockers in heart failure: focus on recent trials with second-generation dihydropyridines. *Am Heart J*. 2000;139:185–194.
26. Ursell PC, Gardner PI, Albala A, Fenoglio JJ Jr, Wit AL. Structural and electrophysiological changes in the epicardial border zone of canine myocardial infarcts during infarct healing. *Circ Res*. 1985;56:436–451.
27. Smith JH, Green CR, Peters NS, Rothery S, Severs NJ. Altered patterns of gap junction distribution in ischemic heart disease. An immunohistochemical study of human myocardium using laser scanning confocal microscopy. *Am J Pathol*. 1991;139:801–821.
28. Gardner PI, Ursell PC, Fenoglio JJ Jr, Wit AL. Electrophysiologic and anatomic basis for fractionated electrograms recorded from healed myocardial infarcts. *Circulation*. 1985;72:596–611.
29. Pagani FD, DerSimonian H, Zawadzka A, Wetzel K, Edge AS, Jacoby DB, Dinsmore JH, Wright S, Aretz TH, Eisen HJ, Aaronson KD. Autologous skeletal myoblasts transplanted to ischemia-damaged myocardium in humans. Histological analysis of cell survival and differentiation. *J Am Coll Cardiol*. 2003;41:879–888.
30. Pogwizd SM, McKenzie JP, Cain ME. Mechanisms underlying spontaneous and induced ventricular arrhythmias in patients with idiopathic dilated cardiomyopathy. *Circulation*. 1998;98:2404–2414.
31. Pogwizd SM, Hoyt RH, Saffitz JE, Corr PB, Cox JL, Cain ME. Reentrant and focal mechanisms underlying ventricular tachycardia in the human heart. *Circulation*. 1992;86:1872–1887.
32. Pogwizd SM, Corr B. The contribution of nonreentrant mechanisms to malignant ventricular arrhythmias. *Basic Res Cardiol*. 1992;87:115–129.
33. Pogwizd SM. Nonreentrant mechanisms underlying spontaneous ventricular arrhythmias in a model of nonischemic heart failure in rabbits. *Circulation*. 1995;92:1034–1048.
34. Menasche P. Skeletal myoblast for cell therapy. *Coron Artery Dis*. 2005;16:105–110.
35. Cheema U, Brown R, Mudera V, Yang SY, McGrouther G, Goldspink G. Mechanical signals and IGF-I gene splicing in vitro in relation to development of skeletal muscle. *J Cell Physiol*. 2005;202:67–75.
36. Guo W, Kamiya K, Yasui K, Kodama I, Toyama J. Paracrine hypertrophic factors from cardiac non-myocyte cells downregulate the transient outward current density and Kv4.2 K+ channel expression in cultured rat cardiomyocytes. *Cardiovasc Res*. 1999;41:157–165.